Catalysis Letters 26 (1994) 9–24

Microwave absorption measurements of the electrical conductivity of small particles

Chan-Chiung Liu, Byung-Ki Na [1], Arden B. Walters and M. Albert Vannice [2]

Department of Chemical Engineering, The Pennsylvania State University, University Park, PA 16802, USA

Received 24 November 1993; accepted 16 February 1994

A microwave absorption technique based on cavity perturbation theory is shown to be applicable for electrical conductivity measurements of both a small, single-crystal particle and finely divided powder samples when σ values fall in either the low ($\sigma < 0.1\ \Omega^{-1}\ cm^{-1}$) or the intermediate ($0.1 \leqslant \sigma \leqslant 100\ \Omega^{-1}\ cm^{-1}$) conductivity region. The results here pertain to semiconductors in the latter region. If the skin depth of the material becomes significantly smaller than the sample dimension parallel to the E-field, an appreciable error can be introduced into the calculated conductivity values; however, this discrepancy is eliminated by correcting for the field attenuation associated with the penetration depth of the microwaves. A modification of this approach utilizing the skin depth allows a first-order correction to be applied to powder samples which results in the accurate measurement of absolute σ values, and results with doped Si powders are compared to σ values obtained from one small single particle using this microwave technique as well as reported DC σ values determined with single crystals. The use of this microwave absorption technique with small particles having high surface/volume ratios, such as catalyst supports and oxide catalysts, under controlled environments can provide fundamental information about adsorption and catalytic processes on such semiconductor surfaces. An application to a ZnO powder demonstrates this capability.

Keywords: microwave absorption; electrical conductivity; single crystal particles; doped Si powders; ZnO powder

1. Introduction

The measurement of electrical properties is vital to the semiconductor industry because of the precision required in the manufacture and application of semiconductor devices [1]. Knowledge of electrical properties is also extremely important for many finely divided solids, such as semiconductor catalysts and catalyst supports, particularly when determining effects of chemisorbed gases and metal–support interactions such as those described by a Schottky barrier. Unfortunately,

[1] Present address: Korea Institute of Science and Technology, Cheongryang, Seoul, Korea.
[2] To whom correspondence should be addressed.

these materials typically are powders comprised of very small particles with high surface/volume ratios. Consequently, the DC and low-frequency AC measurement techniques routinely used with large amorphous particles and single crystals become inapplicable, or at least very complicated, because electrodes cannot be attached to an individual particle and because charge carrier hopping across grain boundaries and inter-particle contacts introduces significant error into measurement of pressed-powder samples [2–4]. The microwave absorption technique is a unique method of measuring conductivity of powder samples which requires no physical electrode contact with the sample and uses a frequency high enough to avoid the necessity of grain boundary or inter-particle charge carrier hopping [4,5]. It also has the advantage of easily allowing a controlled environment for surface chemistry and catalysis experiments when the sample tube is connected to a UHV gas adsorption system [4].

A cavity perturbation method at microwave frequencies has been used to measure electrical properties of CdTe [6], superionic conducting glass [7], germanium [8], superconducting $YBa_2Cu_2O_7$ with Gd [9], as well as other materials [10,11]. Recently, this method has also been applied to calculate microwave dielectric and magnetic parameters [12]. Compared to the DC method, this microwave absorption method for measuring electrical conductivity has the following advantages: (1) the current flow pattern is less dependent on the sample geometry, (2) both surface and bulk electrical properties are measured because the microwave radiation penetrates throughout the sample, (3) problems of ohmic contact voltage between the sample and the electrode can be eliminated, and (4) absolute values can be obtained with powders because charge carrier hopping across grain boundaries and inter-particle contact can be avoided or minimized. Furthermore, when combined with charge carrier mobility measurements in the same cavity using a microwave Hall effect technique, charge carrier densities can also be calculated [4,13].

Based on cavity perturbation theory describing the perturbation of electromagnetic waves inside a resonant cavity induced by a sample possessing a dielectric constant [14], equations relating the conductivity, σ, to measurable cavity properties can be derived for: (1) a low conductivity region with $\sigma < 0.1\ \Omega^{-1}\ cm^{-1}$, (2) an intermediate conductivity region with $0.1 \leqslant \sigma \leqslant 100\ \Omega^{-1}\ cm^{-1}$, and (3) a skin-depth region with $\sigma > 100\ \Omega^{-1}\ cm^{-1}$ [15–19]. This paper describes both the derivation of the equations required to make these measurements and the application of these equations to determine the conductivity of various well-characterized, doped Si single-crystal semiconductor particles as well as Si powder samples to verify the suitability of this technique for finely divided solids. Thus, this technique can study surface phenomena when materials such as catalyst supports and oxide catalysts with high surface areas, i.e., high surface/volume ratios, are utilized.

2. Experimental

The design and construction of the bimodal TE102 rectangular cavity and the

bimodal TE112 cylindrical cavity have been described previously [4,5,13]. These cavities have been used not only to measure conductivity, but also to determine mobility using the microwave Hall effect technique [4]. Doped silicon semiconductors are very well characterized and their mobility and conductivity values as a function of impurity concentration can be obtained from correlations in the literature [20–23]. Therefore, single-crystal Si semiconductor samples with different known DC conductivities were used to verify the applicability of the derived conductivity equations in our two microwave cavities. The reported conductivities of these Si semiconductors ranged from 0.35 to 100 Ω^{-1} cm^{-1}; consequently, the intermediate conductivity equation should be the most appropriate to use. However, when a sample becomes thicker than the microwave skin depth, this equation alone is not sufficient to give an accurate conductivity value, and a penetration depth correction must be implemented to compensate for the attenuation of the intensity of the microwave E-field inside the sample.

The bimodal cavities were connected to a network analyzer (Hewlett-Packard, model 8720) as described previously [5,13], and the resonance spectra of S-parameters were recorded with a Hewlett-Packard Color Pro plotter. The network analyzer was also used to determine the power levels during mobility measurements. Both a bimodal TE112 cylindrical cavity and a TE102 rectangular cavity were used, and the tuning procedures for the cavities have been given earlier [5,13]. The Q_0 and f_0 values were recorded with an empty quartz tube inserted into the microwave cavity.

Well-characterized single-crystal wafers of n-type and p-type Si semiconductors were obtained from the Department of Engineering Science and Mechanics at Penn State University (samples #1–#6) and from Monsanto Electronic Materials Company (samples #7 and #8) so that our measured electrical conductivities could be compared to the reported DC values. However, some of the Si semiconductors obtained still had a certain degree of uncertainty associated with the measured DC conductivities given by the manufacturers; these uncertainties are noted in table 1, which lists the characteristics of the eight semiconductor samples used in this study. The thickness of the Si semiconductors varied from 0.35 to 1 mm. For the single crystal samples, near-square pieces with dimensions of 1.0–3.0 mm were cut from these wafers with a diamond saw. A specially prepared #7 sample was cut into a 1 mm cube which was immersed in an etching solution for 2 min to remove any dangling bonds from the surface. The etching solution was prepared by mixing 70 parts (by volume) nitric acid, 3 parts hydrofluoric acid, and 27 parts distilled, deionized water. This concentration gives an etching rate of about 1 μm/min [24]. Each single-crystal sample was loaded into a 5.0 mm o.d. quartz tube (Wilmad, 703-PQ) and supported on foamed plastic. For the powder samples, the semiconductor samples were first crushed into fine powders using a mortar and pestle, then they were sieved through either a 325 mesh (43 μm) or a 200 mesh (74 μm) wire cloth sieve. All but one semiconductor powder (#7) were treated in etching solution according to the above procedure and loaded into a modified

Table 1
Reported properties of doped Si semiconductor samples

Sample #	Type (orientation)	Dopant conc. [a] N (cm^{-3})	DC conductivity [b] σ_{DC} (Ω^{-1} cm^{-1})	Wafer thickness (mm)
1	Si-P n(100)	2.0×10^{15}	0.37	0.376
2	Si-P n(100)	9.0×10^{15}	$1.6 \pm 25\%$	0.345
3	Si-P n(100)	1.5×10^{18}	$50 \pm 5\%$	0.516
4	Si-B p(100)	2.5×10^{15}	$0.20 \pm 100\%$	0.597
5	Si-B p(100)	8.5×10^{16}	3.3	0.368
6	Si-B p(100)	5.0×10^{18}	$100 \pm 100\%$	0.508
7	Si-P	1.7×10^{15}	0.35	1.0
8	Si-Sb	1.8×10^{18}	59	0.64

[a] Obtained from refs. [20,21] by correlating reported σ_{DC} value (average) to dopant concentration, intrinsic charge carrier density for Si is $10^{10}/cm^3$ so is negligible in contribution to overall charge carrier density.
[b] With uncertainties when appropriate.

5.0 mm o.d. quartz tube containing a circular quartz disc to support the powder. Since a quartz tube distorts the microwave field and Q-factor of the cavity, we used these sample tubes manufactured with precisely controlled dimensions to achieve reproducible sensitivity when insertion and rotation were carried out. The sample tube was located at the antinode of the microwave cavity E-field in the same orientation used for mobility measurements. This positions the sample equally in both modes of the rectangular or cylindrical bimodal cavities; only the primary mode is relevant to conductivity measurements which are performed without any DC magnetic field. When samples were moved toward the E-field antinode at center of the cavity, the resonant frequency of the cavity shifted to a lower value. The sample was considered to be properly positioned when the resonant frequency reached its minimum value. The resonance condition also changed when the sample was rotated, but when the sample was aligned with its longest dimension in the same direction as the microwave field, reproducible results could be obtained.

For conductivity measurements a network analyzer was used to determine cavity Q-factors and resonant frequencies from spectra such as that shown in fig. 1. The spectrum represents reflected microwave power at the microwave primary (inlet) mode. The quality factor of the cavity, Q, is defined by

$$Q = \frac{f_0}{\Delta f_{3dB}}, \tag{1}$$

where f_0 is the resonant frequency, indicated by marker 1, and Δf_{3dB} is the

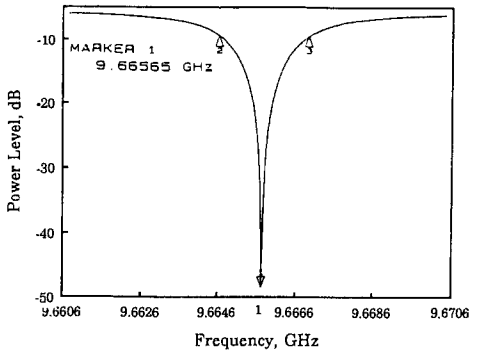

(a)

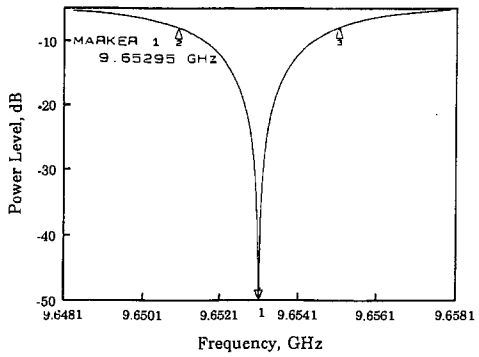

(b)

Fig. 1. Typical resonance spectra for microwave conductivity measurement using a bimodal TE102 rectangular cavity. The spectrum represents reflected power versus frequency in the cavity: (a) spectrum of empty sample tube, (b) spectrum of sample #2 (2 × 2) in sample tube. Marker 1 (resonant frequency) notes the position of maximum attenuation (strongest absorption) of the incident microwave power. Markers 2 and 3 designate the 3 dB power absorption levels relative to the baseline which is an average of −5.5 dB over the entire frequency range. Note the resonant frequency shifts to a lower value, while the resonance spectrum becomes broader (lower Q-factor) when sample is loaded in the sample tube.

frequency difference at a 3 dB power absorption level, relative to the baseline, and is designated by markers 2 and 3. The sample volume was obtained by measuring the weight of each piece and dividing it by the density of Si (2.33 g/cm^3).

3. Results and discussion

Cavity perturbation theory applies a quasi-static approximation, that is, it assumes the microwave field is reduced in intensity but is uniform inside the sample [14]. The electric field inside the sample, E', can be described by the formula

$$E' = \frac{E}{1 + N(\varepsilon - 1)}, \tag{2}$$

where E is the intensity of the electric field impinging on the sample. The cavity perturbation equations provide a relationship between the shift in resonant frequency caused by the sample and the sample dielectric constant [13,15–17]:

$$1 + \frac{N}{\alpha}\frac{\Delta\omega}{\omega_0} = \frac{1 + N(\varepsilon' - 1)}{[1 + N(\varepsilon' - 1)]^2 + (N\varepsilon'')^2}, \tag{3}$$

$$\frac{N}{\alpha}\Delta\left(\frac{1}{2Q}\right) = \frac{N\varepsilon''}{[1 + N(\varepsilon' - 1)]^2 + (N\varepsilon'')^2}. \tag{4}$$

Here ε' and ε'' are the real and imaginary parts of the sample dielectric constant, ε (the relative permittivity), α is the filling factor representing the ratio of the energy stored in the sample to that in the entire cavity, N is the depolarization factor in the direction of the polarized E-field, and $\Delta\omega = \omega - \omega_0$, where ω_0 is the angular resonant frequency of the unloaded cavity and ω is the resonant frequency with the sample present (perturbed). The filling factor is defined as

$$\alpha = \frac{\int |E_i|^2 \, \mathrm{d}V_s}{2\int |E_0|^2 \, \mathrm{d}V_c}, \tag{5}$$

where the numerator and the denominator are volume integrals of the sample and the cavity, respectively [14,16,17].

Simplifications in the cavity perturbation equations can be made, based on appropriate assumptions, to obtain equations applicable to either the low or the intermediate conductivity regions. The dielectric constant is represented by

$$\varepsilon = \varepsilon_0(\varepsilon' - j\varepsilon''), \tag{6}$$

where $\varepsilon_0 = 8.85 \times 10^{-12}$ F/m is the permittivity of a vacuum and ε'' is expressed as

$$\varepsilon'' = \frac{\sigma}{\omega\varepsilon_0} = \frac{\sigma}{2\pi f \varepsilon_0}, \tag{7}$$

where f is the resonant frequency of the cavity ($\omega/2\pi$). For low conductivity samples which have a small dielectric constant [15]

$$N\varepsilon'' < N(\varepsilon' - 1) << 1, \tag{8}$$

which leads to the equation applicable in the low conductivity region

$$\sigma = 2.78 \times 10^{-13} f\left(\frac{Q_0 - Q_L}{Q_0 Q_L}\right)\frac{1}{\alpha}, \tag{9}$$

where Q_0 and Q_L are the quality factors of the unloaded and loaded cavity, respectively [25–28]. In the intermediate conductivity region, ε'' is typically larger than ε', i.e.,

$$N\varepsilon'' > N(\varepsilon' - 1) >> 1 \tag{10}$$

and eqs. (3) and (4) then simplify to

$$\frac{\Delta\omega}{\omega_0} = \frac{\alpha}{N} \tag{11}$$

and

$$\sigma = 1.11 \times 10^{-12} f \left(\frac{\alpha}{N}\right)^2 \left(\frac{Q_0 Q_L}{Q_0 - Q_L}\right) \frac{1}{\alpha} . \tag{12}$$

A filling factor of $\alpha = 2.1 V_s / V_c$ can be derived for a TE112 cylindrical cavity and $\alpha = 2 V_s / V_c$ can be derived for a TE102 rectangular cavity, where V_s is the sample volume and V_c is the cavity volume. The detailed derivations are included elsewhere [34].

We have previously utilized eq. (9) to successfully measure the electrical conductivities of ZnO powders, which have low conductivities [29]. Table 2 lists the conductivity values of our single-crystal semiconductor samples calculated from eqs. (11) and (12) using the data obtained with the bimodal TE112 cylindrical cavity (fig. 2). With an empty quartz tube loaded into the cavity, $Q_0 = 4892$, $f_0 = 9.34315$ GHz, and $V_c = 23.94$ cm^3. The first column of the conductivity values represents the results using eqs. (11) and (12) without the skin-depth correction method which will be discussed later. Reported conductivity values by DC measurements are included in the third column for comparison. Different sizes of sample #5 were examined in order to study the effect of sample size on conductivity

Table 2
Conductivity values of Si semiconductors measured by the microwave absorption technique using a bimodal cylindrical TE112 cavity. The first column of σ values was calculated assuming a uniform E-field, the second column was obtained using the iterative skin-depth correction procedure. For this cavity, $V_c = 23.94$ cm^3, $Q_0 = 4892$, and $f_0 = 9.34315$ GHz

Sample # (dimension) (mm)	Experimental values				α/N [a]	Conductivity, σ (Ω^{-1} cm^{-1})		
	sample thickness (mm)	V_s (cm^3)	Q_L	f (GHz)		eq. (12) (without correction)	eq. (12) (with skin-depth correction)	reported DC values [b]
1 (1 × 1)	0.376	0.8×10^{-3}	2317	9.3374	0.62×10^{-3}	0.26	0.32	0.37
2 (2 × 2)	0.345	1.5×10^{-3}	2613	9.3293	1.48×10^{-3}	1.0	1.5	1.6
3 (3 × 3) [c]	0.516	4.3×10^{-3}	3027	9.2940	5.20×10^{-3}	8.8	76	50
4 (1 × 1)	0.597	1.2×10^{-3}	1991	9.3383	0.51×10^{-3}	0.10	0.12	0.20
5 (1 × 1)	0.368	0.8×10^{-3}	4344	9.3390	0.44×10^{-3}	1.2	1.9	3.3
5 (2 × 2)	0.368	1.4×10^{-3}	3262	9.3308	1.32×10^{-3}	1.5	2.5	3.3
5 (3 × 3)	0.368	3.5×10^{-3}	1281	9.3031	4.29×10^{-3}	1.1	1.8	3.3

[a] Calculated using eq. (11) and $\alpha = 2.1 V_s / V_c$.
[b] Average value from table 1.
[c] Measurement carried out with $Q_0 = 4130$ and $f_0 = 9.3426$ GHz.

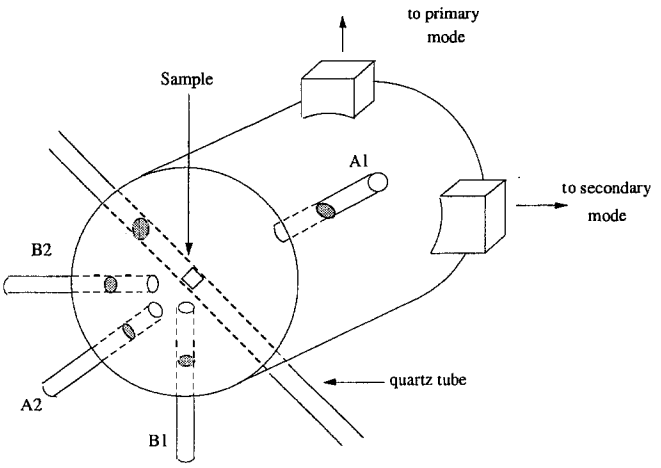

Fig. 2. Schematic drawing of the bimodal TE112 cylindrical cavity and sample tube positioning. A, B represent cavity tuning screws.

measurements. To test the consistency of conductivity values obtained in different cavity configurations, a bimodal TE102 rectangular cavity (fig. 3) was also used and these results are listed in table 3. With an empty quartz tube in the cavity, $Q_0 = 4559$, $f_0 = 9.665975$ GHz, and $V_c = 30.19$ cm^3. Again, the conductivity values obtained by using eqs. (11) and (12) are compared with the measured DC values.

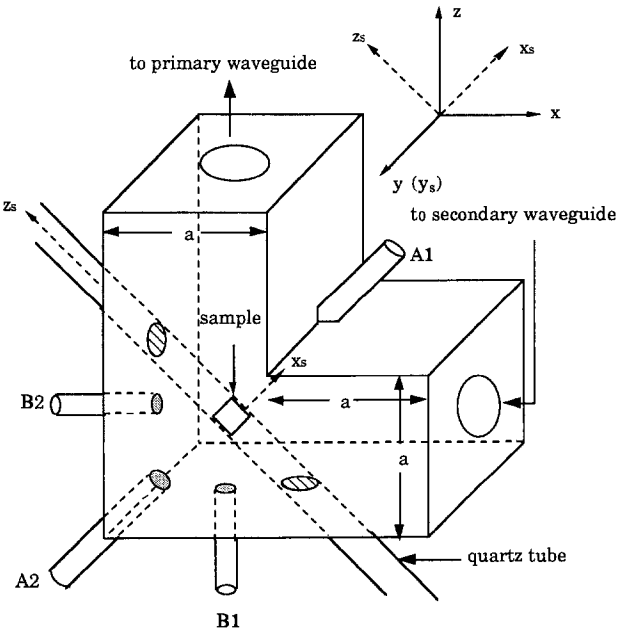

Fig. 3. Schematic drawing of the bimodal TE102 rectangular cavity and sample tube positioning. A, B represent cavity tuning screws. Also shown are the coordinates of both the cavity (x, y, z) and the samples (x_s, y_s, z_s).

Table 3
Conductivity values of Si semiconductors using a bimodal rectangular TE102 cavity. The first column of σ values was calculated assuming a uniform E-field, whereas the second column was obtained using the iterative skin-depth correction procedure. For this rectangular cavity, $V_c = 30.19$ cm^3, $Q_0 = 4559$, and $f_0 = 9.665975$ GHz

Sample # (dimension) (mm)	Experimental values				α/N [a]	Conductivity, σ (Ω^{-1} cm^{-1})		
	sample thickness (mm)	V_s (cm^3)	Q_L	f (GHz)		eq. (12) (without correction)	eq. (12) (with skin-depth correction)	reported DC values [b]
1 (2 × 2)	0.376	1.6×10^{-3}	1590	9.6546	1.17×10^{-3}	0.34	0.43	0.37
2 (2 × 2)	0.345	1.5×10^{-3}	2790	9.6545	1.19×10^{-3}	1.1	1.6	1.6
3 (3 × 3)	0.516	4.3×10^{-3}	3635	9.6333	3.38×10^{-3}	7.7	60	50
4 (1 × 1)	0.597	1.2×10^{-3}	2118	9.6603	5.83×10^{-4}	0.19	0.24	0.20
5 (2 × 2)	0.368	1.4×10^{-3}	3424	9.6557	1.06×10^{-3}	1.7	3.2	3.3
6 (3 × 3) [c]	0.508	4.4×10^{-3}	3595	9.6335	3.43×10^{-3}	9.5	89	100

[a] Calculated using eq. (11) and $\alpha = 2V_s/V_c$.
[b] Average value from table 1.
[c] Measurement carried out with $Q_0 = 4292$ and $f_0 = 9.6665875$ GHz.

From the results in tables 2 and 3, it is clear that the equations derived for the intermediate conductivity region provide good agreement for semiconductors #1, #2, #4 and #5, which are at the low end of this conductivity region, regardless of the type of cavity. However, for samples #3 and #6 which have higher conductivities, the calculated conductivities are much smaller than the DC values. This is due to the attenuation of the E-field within these higher conductivity crystals. A correction related to the penetration depth of the E-field in these samples is required, as described shortly. The equations derived for the intermediate conductivity region appear applicable to the Si semiconductors with the lowest conductivities, even without a penetration-depth correction. One way to verify their applicability is to examine the validity of eq. (11), i.e., $\alpha/N = \Delta\omega/\omega_0$, because it represents a condition that must be fulfilled before eq. (12) can be derived. Since α is known for the two types of cavity used, experimental values of the sample depolarization factor, N, can be calculated from the relationship

$$N_{\text{exp}} = \frac{\alpha}{\alpha/N} = \frac{\alpha}{\Delta\omega/\omega_0} . \tag{13}$$

The theoretical depolarization factor is a function of geometry only, and for these near-square single crystal samples, the depolarization factor can be calculated by the following equation:

$$N_{\text{theor}} = \frac{1}{2(m^2-1)} \left[\frac{m^2}{(m^2-1)^{1/2}} \sin^{-1}\left(\frac{(m^2-1)^{1/2}}{m} \right) - 1 \right], \tag{14}$$

where $m = a/c$, the ratio of the side of the square of the crystal to the specimen thickness [30]. The comparisons of the N_{exp} and N_{theor} values for the cylindrical and rectangular cavities are given in tables 4 and 5. They show that the assumption made for the intermediate conductivity region, $N\varepsilon'' > N(\varepsilon' - 1) >> 1$ which leads to $\alpha/N = \Delta\omega/\omega_0$, is indeed appropriate and yields satisfactory measured σ values.

The calculated conductivities for samples #3 and #6 do not agree well with the DC measurements because the microwave skin depth for these two materials is significantly smaller than the sample thickness; consequently, the E-field inside the sample cannot be assumed to be constant. In this case, the microwave intensity is noticeably attenuated inside the sample so that the E-field-induced (perturbed) parameters such as the Q-factor and the resonant frequency, f, can no longer be considered to be those represented by a sample with a constant or near-constant E-field throughout the sample volume. However, this complication can be removed by using the definition of the filling factor in eq. (5) and modifying the volume integral for the sample to include the E-field attenuation due to the small skin depth of higher conductivity solids. Skin depth is defined as the distance into the conducting medium the microwave E-field must pass to have its amplitude decrease to 1/e of its value at the outer surface of that medium [31,32]; consequently, the classical skin depth is calculated from the following equation:

$$\delta = \left(\frac{2}{\omega\mu_0\sigma}\right)^{1/2} = \left(\frac{2}{2\pi f\mu_0\sigma}\right)^{1/2}, \tag{15}$$

where δ is the skin depth at microwave frequency f and μ_0 is the permeability of a vacuum ($4\pi \times 10^{-7}$ H/m). As microwaves penetrate the sample, the E-field within the sample, E_i, varies as

Table 4
Comparison of experimental values of the depolarization factor, N_{exp}, with theoretical values, N_{theor}. The α/N values were calculated using eq. (11) and $\alpha = 2.1V_s/V_c$. Data were taken from table 2 for the cylindrical TE112 cavity

Sample notation	Sample weight (mg)	Approx. dimension (x_s, z_s, y_s) [a] (mm)	α/N	N_{exp} [b]	N_{theor} [c]	N_{exp}/N_{theor}
1 (1 × 1)	1.9	1.4 × 1.5 × 0.376	0.615×10^{-3}	0.111	0.149	0.745
2 (2 × 2)	3.4	2.2 × 2.2 × 0.345	1.482×10^{-3}	0.082	0.102	0.804
3 (3 × 3)	10.0	2.9 × 3.1 × 0.516	5.202×10^{-3}	0.069	0.111	0.622
4 (1 × 1)	2.7	1.4 × 1.6 × 0.597	0.519×10^{-3}	0.187	0.205	0.912
5 (1 × 1)	1.8	1.4 × 1.4 × 0.368	0.442×10^{-3}	0.145	0.154	0.942
5 (2 × 2)	3.3	2.0 × 2.3 × 0.368	1.322×10^{-3}	0.090	0.110	0.818
5 (3 × 3)	8.1	2.8 × 3.0 × 0.368	4.287×10^{-3}	0.068	0.086	0.791

[a] Dimensions referred to sample coordinates.
[b] $N_{exp} = \alpha/(\alpha/N) = (2.1V_s/V_c)/(\Delta\omega/\omega_0)$.
[c] Calculated using eq. (14).

Table 5
Comparison of experimental values of the depolarization factor, N_{exp}, with theoretical values, N_{theor}. The α/N values were calculated using eq. (11) and $\alpha = 2V_s/V_c$. Data were taken from table 3 for the rectangular TE102 cavity

Sample notation	Sample weight (mg)	Approx. dimension (x_s, z_s, y_s) [a] (mm)	α/N	N_{exp} [b]	N_{theor} [c]	N_{exp}/N_{theor}
1 (2 × 2)	3.6	2.2 × 2.2 × 0.376	1.117×10^{-3}	0.087	0.110	0.791
2 (2 × 2)	3.4	2.2 × 2.2 × 0.345	1.187×10^{-3}	0.081	0.102	0.794
3 (3 × 3)	10.0	2.9 × 3.1 × 0.516	3.380×10^{-3}	0.084	0.111	0.757
4 (1 × 1)	2.7	1.4 × 1.6 × 0.597	0.587×10^{-3}	0.131	0.205	0.639
5 (2 × 2)	3.3	2.0 × 2.3 × 0.368	1.063×10^{-3}	0.089	0.110	0.809
6 (3 × 3)	10.3	3.1 × 3.4 × 0.508	3.425×10^{-3}	0.085	0.103	0.825

[a] Dimensions referred to sample coordinates.
[b] $N_{exp} = \alpha/(\alpha/N) = (2V_s/V_c)/(\Delta\omega/\omega_0)$.
[c] Calculated using eq. (14).

$$E_i = E_{0,max} \exp\left(-\frac{y}{\delta}\right), \tag{16}$$

where y is the distance perpendicular to the sample surface and $E_{0,max}$ is the E-field strength at the surface, i.e., with no attenuation due to skin depth or it can be viewed as the incident microwave E-field strength. Thus the skin depth represents the attenuating effect on the E-field due to the conducting medium.

A one-dimensional correction for the penetration depth is applied here for the following reason. Consider the simplest case in which a near-square, single-crystal sample is located inside a TE102 rectangular cavity. Starting with the standing wave patterns in a particular cavity [33], it can be shown that the only nonvanishing E-field inside this cavity is

$$E_y = E_{0,max} \sin\frac{\pi x}{a} \sin\frac{2\pi z}{d}, \tag{17}$$

i.e., the E-field inside the cavity is polarized along the y-axis [34]. The sample is inserted so that it is oriented in the xz-plane with its flat surface perpendicular to the y-axis. Since the E-field oscillates only in the y direction, the only skin-depth parameter that has to be considered to compensate for the attenuation due to the penetration depth is along the y-axis, i.e., the sample thickness. Sample dimensions in either the x or z direction will generate changes which are included in the experimental parameters such as Q and f. By introducing the correction for penetration depth into eq. (5), the integral for the sample volume becomes

$$\begin{aligned}\int |E_i|^2 \, dV_s &= 2 \int_0^{T/2} \left| E_{0,max} \exp\left(-\frac{y}{\delta}\right) \right|^2 A \, dy \\ &= V_s |E_{0,max}|^2 \frac{\delta}{T} \left[1 - \exp\left(-\frac{T}{\delta}\right)\right],\end{aligned} \tag{18}$$

where A is the cross-sectional area of the sample (area in the xz-plane) and T is the sample thickness (y). The filling factor for the intermediate conductivity region then becomes

$$\alpha_1 = \frac{KV_s}{V_c}\frac{\delta}{T}\left[1 - \exp\left(-\frac{T}{\delta}\right)\right], \tag{19}$$

where K is 2.1 for a TE112 cylindrical cavity and 2 for a TE102 rectangular cavity, and the penetration depth correction factor is defined as

$$\frac{\alpha_1}{\alpha_0} = \frac{\delta}{T}\left[1 - \exp\left(-\frac{T}{\delta}\right)\right]. \tag{20}$$

For the intermediate conductivity region, eq. (12) can be modified by substituting α_1 from eq. (19) for α. This approach results in very good agreement between the σ values calculated from the microwave absorption method and the DC conductivity values for the single-crystal Si semiconductors characterized in this study. Fukuroi and Yamagata have used a similar approach to correct for sample size effects in their calculated dielectric constants for germanium [8].

There is a complication in applying this penetration depth correction to unknown samples because the skin depth is not an independently measurable value; instead, it depends on the electrical conductivity of the sample. Thus, neither the skin depth nor the conductivity can be calculated without knowing the other. However, this difficulty can be overcome by a simple iteration method using the following procedure: (1) a conductivity value, σ_0, is calculated from eq. (12) using $\alpha_0 = 2V_s/V_c$ or $2.1V_s/V_c$, depending on the type of cavity; (2) a skin depth, δ_0, calculated from eq. (15) using σ_0; (3) α_1 is calculated from eq. (19) using δ_0 and T, and it is substituted into eq. (12); (4) a new conductivity, σ_1, is obtained; (5) if the relative deviation $|\alpha_1 - \alpha_0|/|\alpha_0|$ is greater than a specified value, 0.05 for example, σ_1 is substituted into eq. (15) and another iteration is done until the error criterion is met. The conductivity values obtained in this manner are those listed in the second column of σ values in tables 2 and 3. These results give excellent agreement for either cavity type, and they show that the intermediate conductivity equation, with appropriate skin-depth corrections, is applicable over the entire region and is independent of sample size (see results for sample #5, for example). As a further demonstration of the consistency of this microwave absorption technique, results for the cubic #7 sample in the rectangular TE102 cavity are listed in table 6. This represents the average of eight values which were obtained after rotating the sample tube 90° each time during two different runs. Since it was a cubic sample, every orientation resulted in two rectangular faces perpendicular to the y-axis which is the direction of the microwave E-field oscillation. It is clear that the σ values represent the expected results as they should be nearly invariant because the penetration depth for each orientation was essentially the same.

To examine the applicability of this technique to powders and to examine the effect of sample size, particles of samples #5 and #7 smaller than 43 μm and

Table 6
Conductivity values for various forms of Si semiconductor samples #5, #7 and #8 using a bimodal rectangular TE102 cavity ($V_c = 30.19$ cm^3). Data for cubic #7 and all powder samples were obtained after rotating the sample tube 90° each time (eight measurements for cubic #7 during two different runs and four for each powder sample) and average values ± their standard deviation are given

Sample #	Sample form	Particle size	Etched	Weight (mg)	Conductivity, σ (Ω^{-1} cm^{-1})	
					microwave (with skin-depth correction) [a]	reported DC values [b]
5	single crystal	3 × 3 × 0.368	no	10.3	4.3	3.3
	powder	<43 μm	yes	3.0	3.3 ± 0.4	3.3
	powder	<43 μm	yes	5.8	3.3 ± 0.1	3.3
7	single crystal	1 × 1 × 1 mm	yes	2.2	0.38 ± 0.11	0.35
	powder	<43 μm	yes	1.4	0.44 ± 0.05	0.35
	powder	<43 μm	no	1.6	0.62 ± 0.01	0.35
8	single crystal	3 × 3 × 0.64	no	15.3	43	59
	powder	<74 μm	yes	10.2	55 ± 2.2	59
	powder	<74 μm	yes	20.0	55 ± 2.4	59

[a] Calculated using eq. (19) and the described iterative procedure.
[b] From table 1.

sample 8 smaller than 74 μm were placed in the tube and characterized, and the results are also in table 6. These experiments were designed to cover the entire range of intermediate conductivity region by choosing these three samples which have conductivity values approximately an order of magnitude different from one another. Four measurements were again taken after rotating the sample tube 90° each time. The correction procedure for skin depth is somewhat different from that described previously for single-crystal samples. In this case we measured the void fraction in the powder bed, which was 0.50 for #5 and #7 and 0.62 for #8, and assumed the E-field would be unaffected between the particles, thus ignoring the void fraction. In other words, the particles were assumed to collapse into a single, void-free cylindrical volume about the axis of the tube with a radius equal to 2 mm (inner radius of the sample tube) × (1− void fraction). As the E-field was impinging on the wall of a cylinder, the radial penetration depth correction factor became

$$\frac{\alpha_1}{\alpha_0} = \frac{1}{R^2}\left\{R\delta - \frac{\delta^2}{2}\left[1 - \exp\left(-\frac{2R}{\delta}\right)\right]\right\}, \tag{21}$$

where R is the radius of the circular cross section. By the iterative procedure described previously, the corrected conductivities were calculated and are compared to the results from single crystals in table 6. These results are in extremely good agreement with the known values for the bulk material. Table 6 shows that the unetched powder (#7) yielded a higher conductivity value, as expected, due to

the surface dangling bonds created during the crushing procedure. It also shows the quantity of sample used is not a critical factor in conductivity measurements. These results again show the need for skin-depth corrections when samples, including powders, with relatively high σ values are used. Regardless, absolute σ values for powders can be accurately measured.

Finally, to demonstrate the applicability of this approach to study surface phenomena on oxides of catalytic interest, a ZnO powder sample (99.999%) with a surface area of 22 m^2/g was characterized [34]. After evacuation at 673 K for 2 h, the conductivity measured in the microwave cavity was $\sigma = 0.082\ \Omega^{-1}\ cm^{-1}$ and the mobility determined by the microwave Hall effect technique (4) was $\mu = 5.1\ cm^2/V\ s$, thus the electron density, $N_c = \sigma/\rho e\mu$, where e is the electron charge and ρ is the density of the ZnO, was $18 \times 10^{15}\ e^-/g$ ZnO. Chemisorption of O_2 at 300 K reduced σ to $0.0049\ \Omega^{-1}\ cm^{-1}$ and increased μ to $44\ cm^2/V\ s$; consequently, the electron density was reduced to $0.12 \times 10^{15}\ e^-/g$ ZnO. After evacuation at 300 K, exposure to 20 Torr CO increased σ to $0.0058\ \Omega^{-1}\ cm^{-1}$, decreased μ to $9.7\ cm^2/V\ s$ and increased the electron density to $1.8 \times 10^{15}\ e^-/g$ ZnO. Thus it is clear that surface processes can be monitored; in this example, chemisorbed O atoms interact with conduction electrons and reduce their density while CO can react with some of these adsorbed O atoms to partially restore conduction electron density.

4. Conclusions

A microwave absorption technique based on cavity perturbation theory has been shown to be applicable for electrical conductivity measurements of either a single-crystal particle or finely divided powder sample when σ values fall in either the low or the intermediate conductivity region. The results here pertain to semiconductors in the intermediate region, i.e., $0.1 \leqslant \sigma \leqslant 100\ \Omega^{-1}cm^{-1}$. A quasi-static approximation was assumed in the derivation of the conductivity equations, i.e., the microwave field is reduced in intensity but remains uniform inside a sample. However, if the skin depth of the sample becomes significantly smaller than the sample dimension parallel to the E-field, this assumption becomes inappropriate and an appreciable error is introduced into the calculated conductivity values. This discrepancy can be remedied by correcting for the attenuation associated with the penetration depth of the microwaves. Through a simple model which describes a non-uniform field caused by effects due to geometry and the intrinsic skin depth, a straightforward iterative procedure is described which gives accurate conductivity values, independent of size. A small modification of this approach allows a first-order correction to be applied to powder samples which results in accurate σ measurements. Consequently, the microwave absorption technique is applicable to powders with either low or intermediate conductivities, and its use with small particles having high surface/volume ratios under controlled environments can provide

much fundamental information about adsorption and catalytic processes on semiconductor surfaces. An example of this is provided by characterizing a high surface area ZnO powder.

Acknowledgement

This research was supported by the Florida Power & Light Company. Funding from an NSF equipment Grant (CBT-8505572) was used to provide the ESR spectrometer. We also appreciate the loan of the Si semiconductor wafers from Professor S.J. Fonash and his group at Penn State and from Dr. J.P. DeLuca, Monsanto Electronic Materials Company.

References

[1] B.R. Nag, G. Ghosh and S. Dhar, Solid-State Electronics 35 (1992) 1823.
[2] T.J. Gray, Measurement of semiconductivity, photoconductivity, and associated properties of catalysts, in: *Experimental Methods in Catalytic Research*, ed. R.B. Anderson (Academic Press, New York, 1968) ch. 7.
[3] K.H. Oh, C.K. Ong and B.T.G. Tan, J. Phys. E 22 (1989) 876.
[4] B.-K. Na, M.A. Vannice and A.B. Walters, Phys. Rev. B 46 (1992) 12226.
[5] B.-K. Na, S.L. Kelly, M.A. Vannice and A.B. Walters, Meas. Sci. Technol. 2 (1991) 770.
[6] M. Godlewski, Phys. Stat. Sol. (a) 51 (1979) K141.
[7] J. Kawamura and Y. Oyama, Solid State Ionics 35 (1989) 311.
[8] T. Fukuroi and K. Yamagata, Sci. Rep. RITU A 11 (1959) 285.
[9] M.D. Sastry, R.M. Kadam, Y. Babu, A.G.I. Dalvi, I.K. Gopalkrishnan, P.V.P.S. Sastry and R.M. Iyer, Physica C 153 (1988) 1667.
[10] E.M. Trukhan, Soviet Phys. Sol. State 4 (1963) 2560.
[11] S. Sen, P.K. Saha and B.R. Nag, Rev. Sci. Instrum. 50 (1979) 1594.
[12] V.R.K. Murthy and R. Raman, Solid State Commun. 70 (1989) 847.
[13] B.-K. Na, PhD Thesis, The Pennsylvania State University, USA (1991).
[14] J.L. Altman, *Microwave Circuits* (Van Nostrand, Princeton, 1964).
[15] N.P. Ong, PhD Thesis, The University of California, Berkeley, USA (1976).
[16] N.P. Ong, J. Appl. Phys. 48 (1977) 2935.
[17] L.I. Buranov and I.F. Shchegolev, Instr. Exp. Tech. 2 (1971) 528.
[18] N.P. Ong, W. Bauhofer and C. Wei, Rev. Sci. Instrum. 52 (1981) 1367.
[19] M. Cohen, S.K. Khanna, W.J. Gunning, A.F. Gartio and A.J. Heeger, Solid State Commun. 17 (1975) 367.
[20] J.C. Irvin, Bell Syst. Tech. J. 41 (1962) 387.
[21] D.M. Caughey and R.E. Thomas, Proc. IEEE 55 (1967) 2192.
[22] W.R. Thurber, R.L. Mattis, Y.M. Liu and J.J. Filliben, J. Electrochem. Soc. 127 (1980) 1807.
[23] W.R. Thurber, R.L. Mattis, Y.M. Liu and J.J. Filliben, J. Electrochem. Soc. 127 (1980) 2291.
[24] P.M. Lenahan and J. Dressendorfer, Appl. Phys. 55 (1984) 3495.
[25] D.D. Eley and R. Pethig, Discussions Faraday Soc. 51 (1971) 164.
[26] E.M. Trukhan, Instr. Exp. Tech. 4 (1965) 947.
[27] M.M. Sayed and C.R. Westgate, Rev. Sci. Instrum. 46 (1975) 1074.
[28] M.M. Sayed, PhD Thesis, The Johns Hopkins University, USA (1972).

[29] B.-K. Na, A.B. Walters and M.A. Vannice, J. Catal. 140 (1993) 585.
[30] J.A. Osborn, Phys. Rev. 67 (1945) 351.
[31] L.C. Shen and J.A. Kong, *Applied Electromagnetism* (PWS Engineering, Boston, 1987).
[32] N.W. Ashcroft and N.D. Mermin, *Solid State Physics* (Holt, Rinehart and Winston, New York, 1976).
[33] C.P. Poole, *Electron Spin Resonance: A Comprehensive Treaty on Experimental Techniques* (Wiley, New York, 1983).
[34] C.-C. Liu, PhD Thesis, The Pennsylvania State University, in progress.